

## Gravity and Microearthquake Studies in the Chinshan-Tanshui Area, Northern Taiwan

KUANG-JUNG CHEN<sup>1</sup> AND YIH-HSIUNG YEH<sup>1</sup>

(Received 30 November 1990; Revised 28 March 1991)

### ABSTRACT

Gravity and microearthquake surveys were carried out in the Chinshan-Tanshui area, northern Taiwan in 1987. Bouguer anomaly data was used to determine the subsurface structures of this area. The results indicate that the Chinshan fault is a thrust fault with a dipping angle of about 55 to 60 degrees. A temporary seismographic network with twelve stations was deployed to study the seismicity of the area. 223 events with magnitudes between 0.2 and 3.2 occurred in the study area during the 58 days survey period. Most of them were at depths shallower than 10 km. From the fault plane solutions, we can see that most of the focal mechanisms in this area are from normal faulting. They must be correspond to the activity of the Tatun and Chishinshan volcanos. 433 earthquakes in the study area were recorded by the Taiwan Telemetered Seismographic Network (TTSN) during the period between 1973-1985. The distribution pattern is quite similar to that revealed by the temporary array. In general, this area shows steady moderately active shallow seismicity.

### 1. INTRODUCTION

Gravity data play an important role in the study of subsurface structures because the lateral variation in density at different depths within the earth will directly affect the gravity on the surface. A fault is a structure which often causes gravity anomalies on ground surface in the area above it. This can be related to lateral variations of density along the profile perpendicular to the fault, therefore, gravity survey will be made along profiles which are perpendicular to the fault. The location and character of the fault can be deduced from the pattern of the Bouguer anomalies.

For delineating the Chinshan fault and the other subsurface structure surrounding this fault, a detailed microgravity survey along three profiles has been carried out in Chinshan-Tanshui area. The data are interpreted to understand the subsurface structures in this area.

---

<sup>1</sup> Institute of Earth Sciences Academia Sinica, Taiwan, Taipei, R. O. C.

Microearthquakes in general occur in large numbers and often have distinct spatial distribution. Seismicity data can be collected in a short intervals of time to delineate the pattern of recent tectonic activity. Thus, through microearthquake survey, one can obtain significant seismologic and tectonic insight in the study area. The main purpose of the present microearthquake investigation are: (1) to understand the current seismicity (2) to ascertain whether there are active faults, and (3) to determine the characteristics of the active faults if they exist.

In order to observe microearthquakes that occurred inside the Chinshan-Tanshui area, a temporary seismographic network composed twelve stations was installed by the Institute of Earth Sciences, Academia Sinica in 1987.

## 2. GEOLOGIC SETTINGS

Early and late Miocene sedimentary rocks and Pleistocene volcanic rocks are exposed in the study area. The early Miocene rocks are the Wuchihshan Formation, the Mushan Formation, and the Talio Formation. The late Miocene rocks are the Nanchuang Formation, and the Kueichulin Formation. The Pleistocene rocks are the Kuanyinshan Formation, Linkou Formation and volcanic breccias. As given by Chang (1968), Chou (1962), Hsu (1967) and Hsu (1981), the surface geologic data in the study area are shown in Fig. 1, and the characteristics of above formations can be summarized as follows:

### 1. Wuchishan Formation:

The maximum thickness of this formation is estimated to be more than 1200 *meters*. Massive white sandstone is predominant in this formation and belongs to the category of orthoquartzite or psotoquartzite.

### 2. Mushan Formation:

This formation is characterized by white, medium- to coarse-grained quartzose sandstones which are mostly psotoquartzite in composition. Only the upper part of this formation with a thickness of 300 *meters* is exposed in the study area.

### 3. Taliao Formation:

The thickness of this formation is about 500–550 *meters*. This formation is a marine unit directly overlying the coal-bearing Mushan Formation. The type locality of this formation bears a monotonous sequence of thick-bedded to massive sandstone alternated with thin and thick beds of shale and silty shale.

#### 4. Nankang Formation:

The total thickness of this formation is about 700 – 750 *meters* in the study area. It is composed of thick- to thin-bedded, light bluish gray, fine-grained calcareous sandstone and dark gray shale or siltstone.

#### 5. Nanchuang Formation:

The total thickness of this formation is 500 to 600 *meters*. This formation is distributed in the southeastern part of the study area. It is composed largely of white sandstone.

#### 6. Kueichulin Formation:

This formation is generally divided into two units, the Tapu Formation below and the Erhchiu Formation above. The Tapu Formation is composed of thick-bedded, light gray muddy sandstone. The thickness of the Tapu Formation is 300 – 400 *meters*. The Erhchiu Formation in the upper part is composed also of thick-bedded, light bluish gray muddy sandstone. The thickness of the Erhchiu Formation is usually 400 to 500 *meters*.

#### 7. Linkou Formation:

This formation comprises all the gravels and the lateritic mantle. The gravel is composed mainly of lithic and quartzitic sandstones. The total thickness of this formation is about 200 *meters*.

#### 8. volcanic rocks:

Volcanic rocks in this area consist of volcanic breccias, andesitic lava flows and andesite detritus. The tuffaceous breccia is widely distributed in the northwestern part of the study area and forms a gently west-dipping platform with a long cliff on the coast. This platform ranges from 50 to 260 *meters* in elevation. The thickness of the tuffaceous breccia is estimated as nearly 120 *meters*. The andesite detritus consists of volcanic ash and weathered andesite blocks which are scattered on the hill slopes.

The known structural features of the study area are the Wanli homocline, the Chinshan fault, the Tiaoshih syncline, and the Kanchiao thrust fault (Hsu, 1967). The Wanli homocline extends from the northwest of the Kanchiao fault to the Huangchi stream and is bounded on the northwest by the Chinshan fault. The Chinshan fault, also termed Hsinchuang fault, is completely concealed under alluvium in the Chinshan valley. The trace of the Chinshan fault shown in Fig. 1 is inferred from the gravity data by Hsu (1967). This fault strikes  $N 56^{\circ} E$  and follows approximately the northwestern edge of the Chinshan valley. It extends inland from the coast near Chungchiao to Huangchitou and

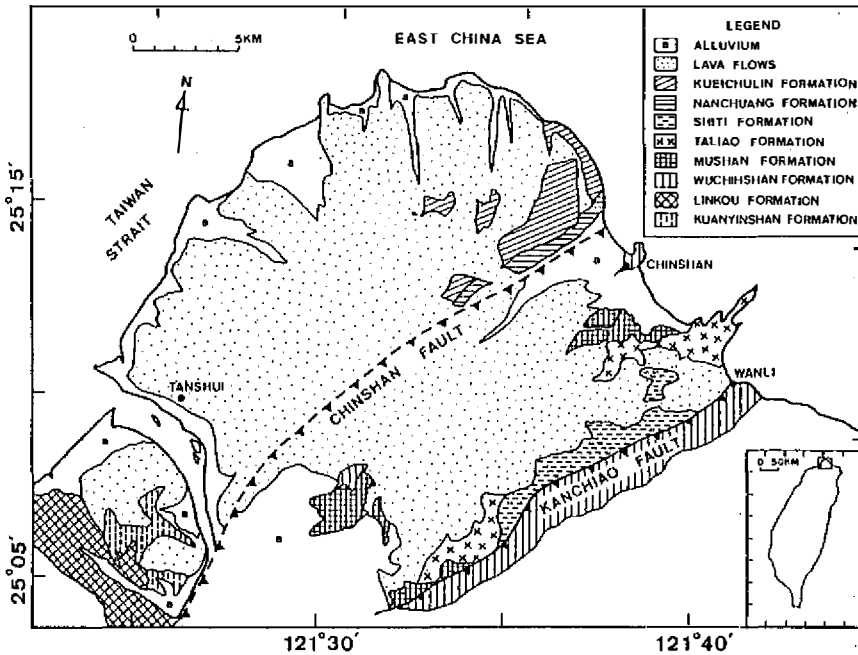


Fig. 1. Simplified geologic structure map of the Chinshan-Tanshui area.

then into the Tatun volcano area. The Chinshan fault is inferred to be a thrust fault dipping to the southeast, the hanging wall being composed of the base of the Wuchihshan Formation and the footwall of the lower part of the Nanchuang Formation. The fault separates the Wanli homocline in the upper block from the Tiaoshih syncline in the lower block. The Tiaoshih syncline is limited on the southeast by the Chinshan fault. The axial trace of the Tiaoshih syncline trends  $S 56^{\circ} W$ . The middle part of this syncline is covered entirely by volcanic breccias and lava flows from the Tatun Volcano Group. The Kanchiao thrust fault strikes  $N 60^{\circ} E$  and follows approximately the Masuchistream from Kanchiao to Wanli and into the sea. The fault plane follows the lower part of the Wuchishan Formation. This fault separates the Wanli homocline in the lower block from the Tawulun homocline in the upper block. The fault plane near the surface dips from  $45^{\circ}$  to  $50^{\circ}$  southeastward.

### 3. GRAVITY STUDY

Two gravity profiles which were essentially perpendicular to the Chinshan fault (as shown in Fig. 2) have been surveyed in this study. The LaCoste-Romberg Model D-48 microgal gravimeter was used in the survey between August 7 and September 16, 1987. The gravity values were tied to the gravity base of the National Central University at Chungli.

The field work of gravity survey and the methods of data analysis are sim-

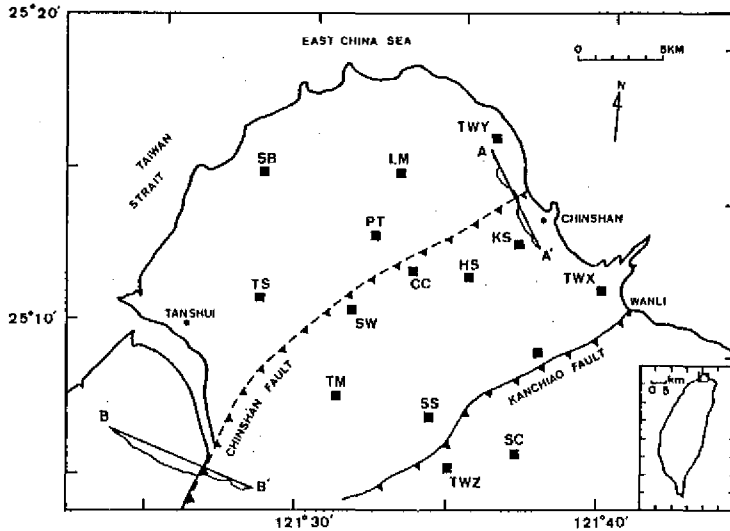


Fig. 2. Gravity profiles ( $AA'$  and  $BB'$ ) and seismographic stations.

ilar to those described by Yeh *et al.* (1984). Field work in this study includes selection of gravity sites, determination of the site location and elevation and measurement of gravity. Gravity sites are selected at points on solid ground. They must be away from any tunnel, bridge or stream. Determination of site locations is done in two ways, most site locations were determined by using 1:5000 scale photographic maps. Their elevations are determined by the closure leveling measurement. When the location of some sites cannot be determined using the photographic maps, the locations and elevations are determined by closure stadia traverse surveying. Nikon NT-3A theodolite is used for both of the leveling measurement and stadia traverse surveying. The reference bases for the geodetic survey were selected at bench marks or triangle points nearby. To make the correct for instrument drift and tidal effect on gravity measurements, the gravity surveys are run on loops. Each loop is completed within an hour. The topographic description within a range of 25 meters surrounding each station is also made. The description will be used for near-distance terrain correction. The gravity measurements are corrected for instrument drift, tidal effect, elevation, terrain and latitude in order to obtain Bouguer gravity anomalies. Corrections of the instrument drift and the tidal effects can be made reasonably well on the assumption that their variations are linear with time within an hour. Elevation correction includes free-air and Bouguer corrections. Free-air corrections are made according to the expression for the vertical gradient  $-0.3086 \text{ mgal/m}$ . Bouguer corrections are made by the formula for an infinite horizontal slab

$$\delta g = 0.04185 \rho H$$

where  $H$  is the height in meters relative to the datum level (e.g. Sea level),  $\rho$

is the average density of strata between gravity station and datum, and  $\delta g$  is the magnitude of Bouguer correction in mgal. In this study the average surface density is assumed as  $2.4 \text{ gm/cm}^3$  based on the study of Hsieh and Hu (1972). Terrain corrections are made principally by Hammer's method (1939). The latitude corrections are made according to the International Gravity Formula which was adopted by the International Union of Geodesy and Geophysics in 1967. After the corrections having been made, the Bouguer anomaly at each station is obtained. For modeling the subsurface structures, the gravity sites along the same profile are usually projected on a proper straight line. In this study, the lines chosen are shown in Fig. 1. The gravity anomaly data projected on each profiles are further smoothed and interpolated to provide equal-spacing data points over the profile. The gravity profiles obtained after those procedures are shown in Figs. 3 and 4.

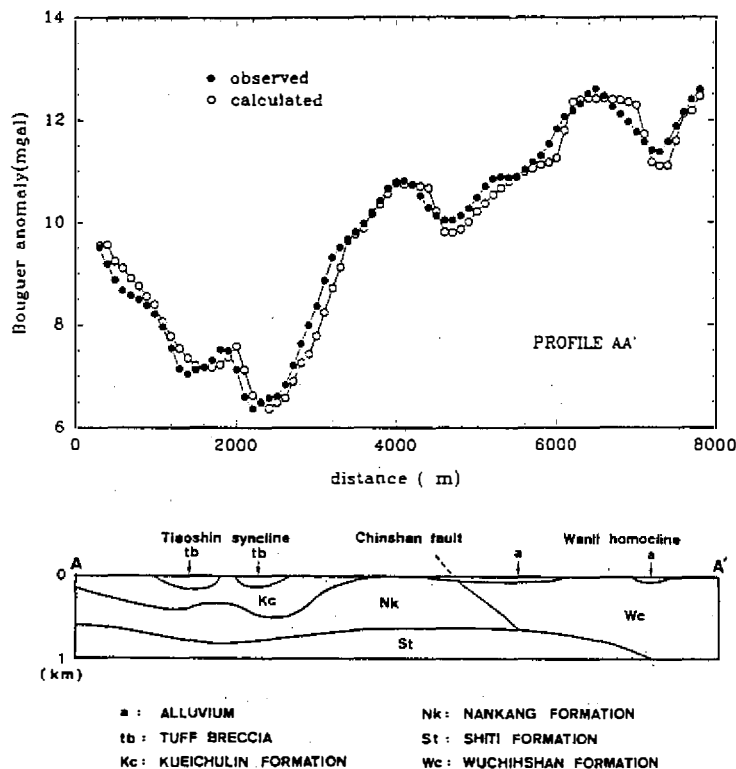


Fig. 3. Result of inferred subsurface structure along AA'(bottom). The calculated (hollow circle) and the observed (solid circle) gravity data are also shown(top).

It is well known that the subsurface density distribution cannot be uniquely determined from gravity (or other potential field) data. However, the difficulty of a nonunique solution can be partially overcome by incorporating or

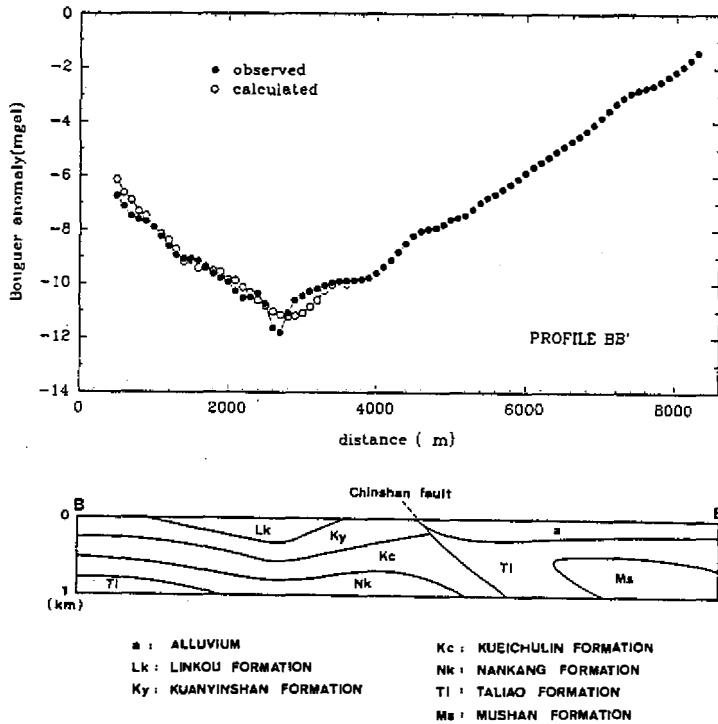


Fig. 4. Result of inferred subsurface structure along  $BB'$  (same format with Fig. 3).

comparing it with geological or other geophysical information. Therefore, geological and other geophysical information in the study area obtained by other authors are used to supplement the gravity data. The information in our study includes a wildcat well in Chienshanhu, 4.5 kilometers south of Shihmen (Hsu, 1967), and the thickness of each formation underlying the gravity profile (Hsu, 1981). The analytic gravitational field formula derived by Talwani *et al.* (1959) is used in calculating the theoretical gravity. In our modeling procedure, a trial and error method is performed iteratively until the observed and calculated gravity values match each other satisfactorily.

Figure 3 shows the result of the inferred model of subsurface structure beneath the profile  $AA'$ . In general, the calculated and observed gravity anomalies agree well, those that don't fit may be due to anomalous bodies at very shallow depths. The results indicate that the Chinshan fault is a thrust fault with a dipping angle of about  $60^\circ$  SE. The hanging wall of this fault is composed of the base of the Wuchihshan Formation and the footwall of the lower part of the Nankang Formation. The Chinshan fault is completely concealed under the alluvium of the Chinshan valley. Northwest of the Chinshan fault, a gentle syncline extending from 0 km to 4 km exists. This syncline is named as Tiaoshih syncline by Hsu (1967). The middle part of this syncline is covered entirely by

volcanic breccias(*tb*) and lava flows of the Tatun Volcano Group. In addition, there is a drag fold within this syncline, which is supposed to be caused by the drag force during the thrust faulting of the Chinshan fault.

Figure 4 shows the inferred model of the subsurface structure along the profile *BB'*. The results indicate that the dip of the Chinshan fault is about 55 degrees. The hanging wall of the fault is composed of the Taliao Formation while the footwall composing the Kuanyinshan Formation, the Kueichulin and the Nankang Formation. The fault plane also defines the north limb boundary of the Shantzechiao anticline.

#### 4. MICROEARTHQUAKE STUDY

A temporary seismographic network of twelve stations was installed in the study area between August 23 and October 18, 1987 (Table 1 and Fig. 5). The network covered about 200  $km^2$ . Each station was equipped with a short-period (1 Hz) vertical seismometer (Mark Products, Model L-4C), a seismographic system, and external batteries. The seismographic system used in this study was MEQ-800 (Sprengnether Instrument Co.) PDR1, and PDR2 (Kinematic Co.) (Table 1). MEQ-800 contains an amplifier, a smoked drum recorder, an accurate chronometer and internal batteries. The signals were recorded on smoked paper that was changed every day. The drum speed was 120  $mm/min$ , and second marks were superimposed on the trace to provide precise timing. Standard radio time code was directly recorded on the seismograms twice a day, i.e., at the beginning and the end of each record, to provide absolute time. The length of a second on the traces was 2  $mm$ . P- and S-wave arrivals on the traces were timed to one hundredth of a second by use of a microscope. Therefore, the P- and S-wave readings have an accuracy of 0.01  $sec$ . The signals recorded in PDR1 or PDR2 are converted to digital type in 12 bits. 1/200 of sampling rate is used in the survey period. So, the P- and S-wave reading have an accuracy of 0.005  $second$ . In order to facilitate more reliable reading of *S* arrivals, a short-period horizontal seismographic unit was deployed alongside with vertical unit at stations Kanchiao (KC), and Pinting (PT). In addition to the 12 temporary stations, data from three TTSN stations near the survey area were also used (TWX, TWY and TWZ) (Fig. 2).

The methods of microearthquake data processing are similar to those of Tsai *et al.* (1975). Events recorded simultaneously by more than four stations were used for data analysis. Locations of earthquakes were determined mainly by the first arrivals of *P* waves. *S* wave arrivals were used to supplement the *P* waves whenever possible. The available arrival time data were subsequently fed into the computer program HYPO71 (Lee and Lahr, 1972) to determine the hypocentral location and origin time of the earthquake by minimizing the residuals between the observed and the theoretical arrival times by the Geiger's

Table 1. Status of seismographic stations

STATION	CODE	LAT-N (°)(')	LON-N (°)(')	ELEVATION (meters)	AMP. (dB)	RECORD SYSTEM
Kanchiao	KC	25°09.73	121°37.63	260	72	MEQ-800
Laomei	LM	25°15.28	121°32.91	140	60	MEQ-800
Pintin	PT	25°13.01	121°32.61	645	72	MEQ-800
Huangshan	HS	25°11.87	121°35.57	345	66	MEQ-800
Chiku	CC	25°11.97	121°33.53	52	66	MEQ-800
Sueiwei	SW	25°10.70	121°31.80	60	60	MEQ-800
Suansee	SS	25°07.50	121°34.10	40	72	MEQ-800
Chinshan	KS	25°13.19	121°36.87	13	72	PDR-1
Shihchih	SC	25°06.20	121°37.20	40	66	PDR-2
Tienmu	TM	25°07.90	121°31.10	95	72	PDR-1
Tanshui	TS	25°10.97	121°28.20	158	60	PDR-2
Siiibang	SB	25°15.20	121°28.10	45	66	PDR-2
Koushen	TWX	25°11.93	121°39.70	40	66	VCO
Chanhwa	TWY	25°16.55	121°35.98	20	66	VCO
Neihu	TWZ	25°05.82	121°34.74	280	54	VCO

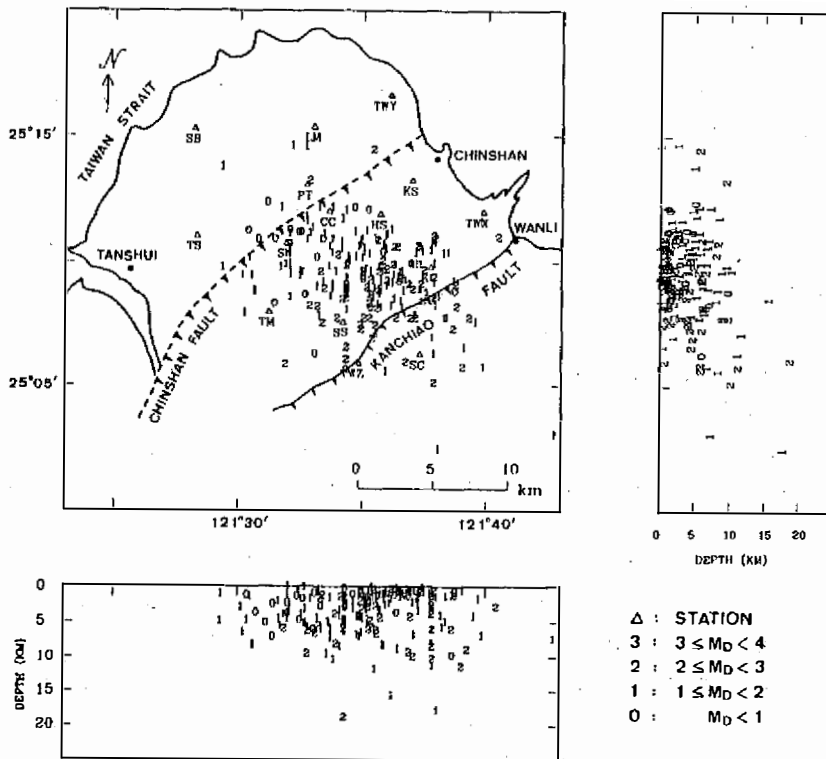


Fig. 5. Epicentral distribution and NS EW cross section of hypocentral locations. Seismographic stations are denoted by hollow triangles.

method (Geiger, 1912). The theoretical arrival times were calculated with the assumption of horizontally layered crust model. The velocity model adopted for the present study was as follows:

Layer	Depth (km)	P-velocity (km/sec)	S-velocity (km/sec)
1	0-9	5.84	3.28
2	9-17	6.07	3.41
3	17-36	6.73	3.78
4	below 36	7.79	4.38

This model was based on Yeh's result (1986). Since the elevation of stations differed as much as 690 meters, an approximately correction of travel time for elevation was made according to the following formula:

$$\delta t = -H/V$$

where  $\delta t$  represents the elevation correction of travel time,  $H$  is the station elevation in meters, and  $V$  is average P-wave velocity of rocks above the sea level in  $m/sec$ . A value of 3000  $m/sec$  for average P-wave velocity was adopted for the present case.

The earthquake magnitude  $M$  was determined from the signal duration by the following formula (Lee *et al.*, 1972)

$$M = -0.87 + 2.0 \log T + 0.0035 \tau$$

where represents  $T$  the total signal duration in second and  $\tau$  represents the epicentral distance in kilometer.

The seismic data recorded by the temporary network allowed us to locate a total of 239 events. The location qualities were evaluated by the root-mean-square error of residuals (RMS). The standard error of epicenter and the standard error of hypocenter's depth, were computed by the computer program HYPO71. Under the restrictions,  $RMS < 0.3 \text{ sec}$ ,  $ERH < 2 \text{ km}$  and  $ERZ < 2 \text{ km}$ , only 223 of events were obtained. Figure 5 shows their epicentral distributions. Two cross sections along  $NS$  and  $EW$ , the hypocentral locations were projected in the same figure. Most of these earthquakes were located within the block bounded by the Chinshan fault and the Kanchiao fault. More than 95% of events occurred at depths shallower than 10  $km$ , obviously condensing in the depth between surface to 5  $km$  deep. The daily frequency of the located earthquakes within the period from August 8 to October 18, 1987, were presented in Fig. 6. On average, about 4 events were located in one day. In addition, we may easily find that the daily frequency can be modulated by

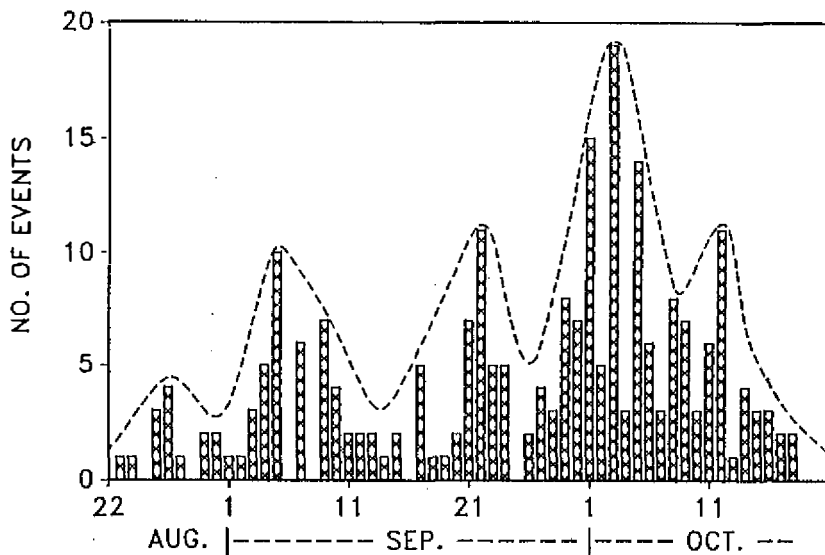
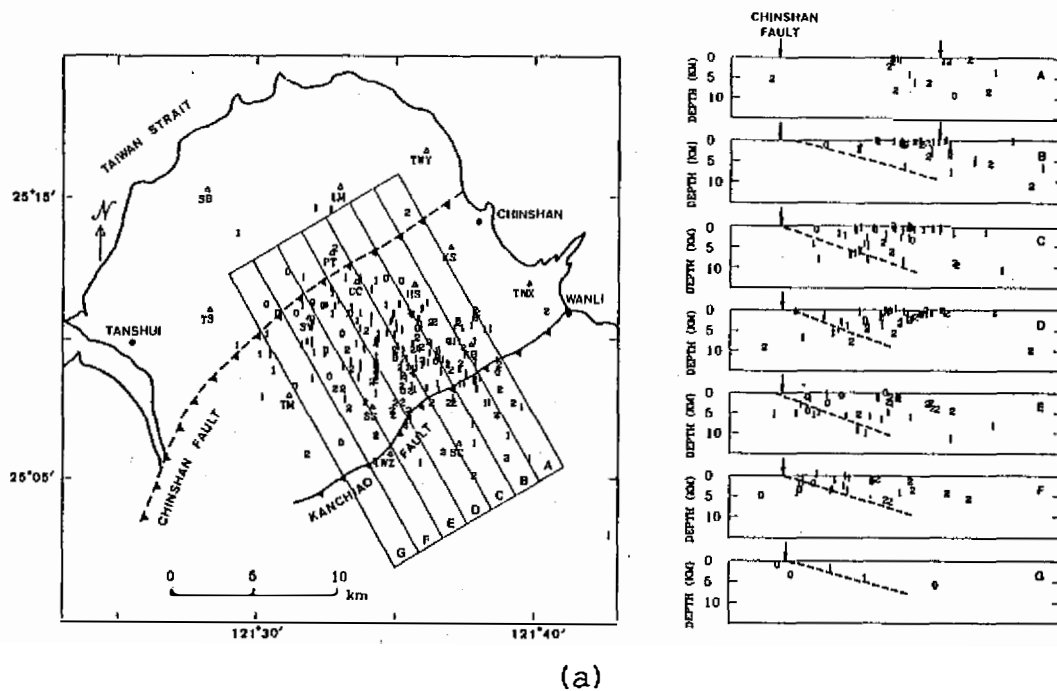


Fig. 6. Statistics of the located events.

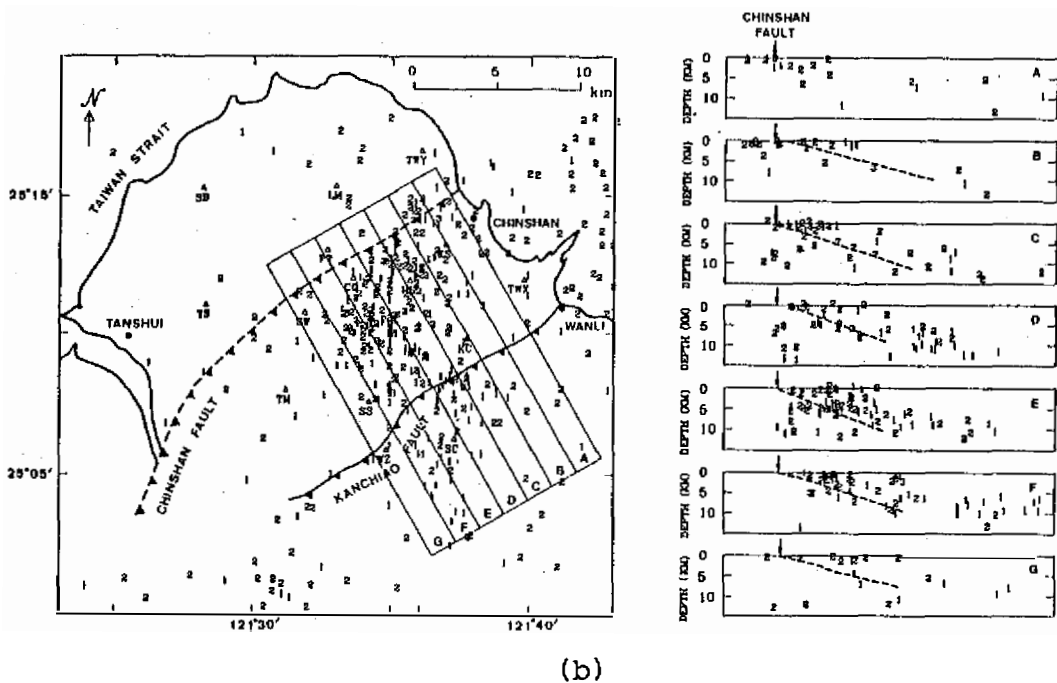
a spline curve (dash line in Fig. 6) with a period of about 10 days. Is this the recurrence period in this area or not? The survey period of this temporary network is too short to ascertain the answer.

To verify a correlation between the active fault and the seismicity in this area, we have examined the spatial distribution of earthquakes that occurred within our study area. Figure 7 shows the hypocentral profiles within each block (denoted by A-G) which is approximately perpendicular to the strike of the Chinshan fault. Most events were shallower than 10 km. A southeast-dipping seismic zone with an angle of about 45° is visible. This angle is similar to the dip angle of the Chinshan fault modeled by gravity data. It implies that the Chinshan fault is unrested. The earthquakes located in this area by the TTSN for the period from 1973 to 1985 are shown by the same format (Fig. 7b). The epicentral distribution is quite similar to that revealed by the microearthquake survey. They also exhibit some epicenters that occurred near the Chinshan fault. The spatial distribution is more or less similar to that obtained by the microearthquake survey.

From the microearthquake data, twenty one composite fault-plane solutions obtained from the polarities of P-wave first motion plots on a stereographic equal-area display are compiled and shown in Fig. 8. (The earthquakes used to construct the fault plane solutions are shown in Fig. 9.) Sixteen of them are normal faults, striking roughly northwest. They probably correspond to the geothermal activities of the Tatun or Chihsinshan Volcanoes. Only one of them is thrust fault (group E). The hypocenters of this earthquake group are located



(a)



(b)

Fig. 7. Hypocentral profiles within each blocks (A-G), occurred (a) during the period Aug. 23-Oct. 18, 1987, and (b) 1973-1985 (TTSN). The vertical axis (depth) were exaggerated by a factor of 4.

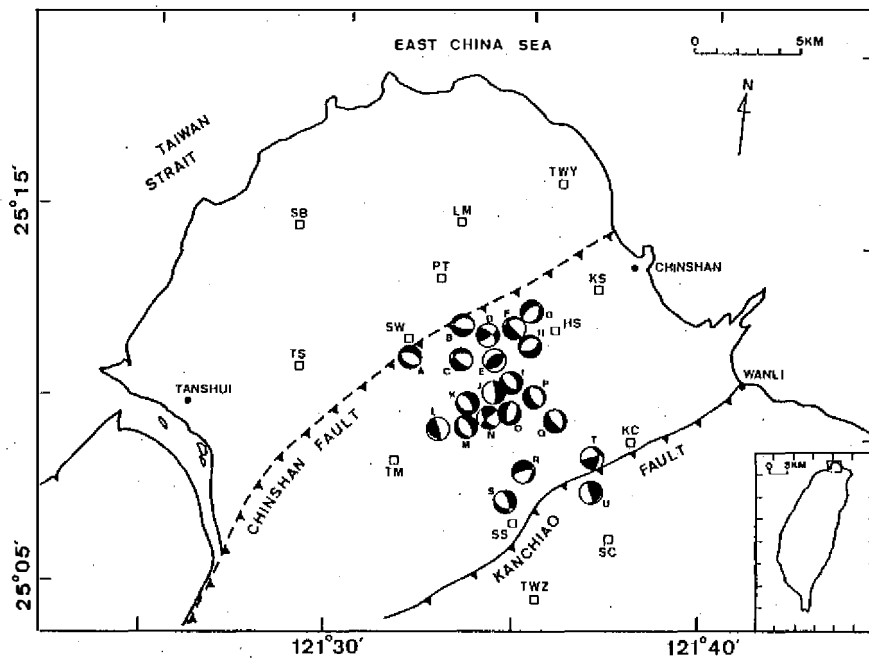


Fig. 8. Composite fault-plane solutions from microearthquake data. The character beside each sphere is the group name.

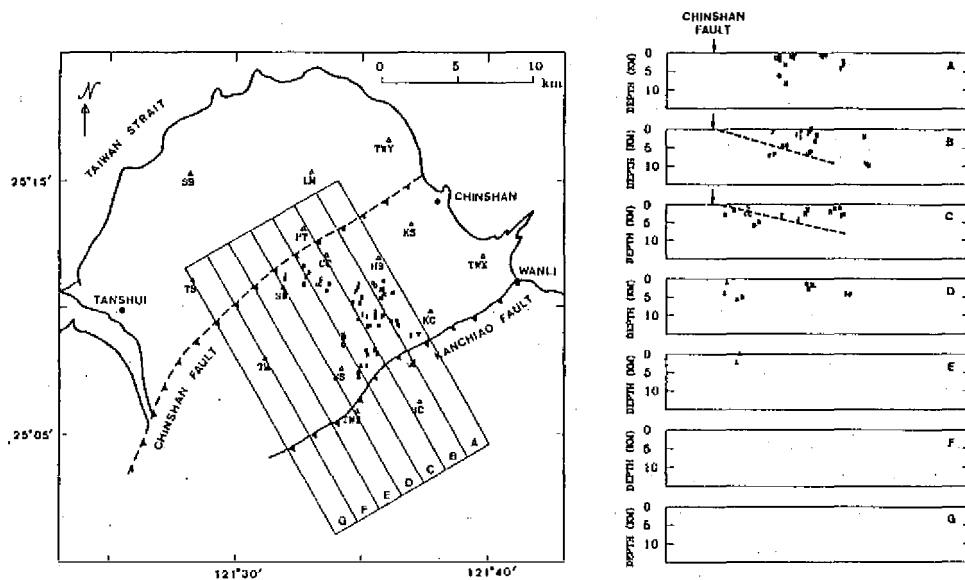


Fig. 9. The earthquakes used to construct the fault plane solutions in Fig. 8 (Each event was denoted by the group name which it belongs to).

near the fault plane of the Chinshan fault. It is believed that these earthquakes may be produced by the activities on the Chinshan fault.

## CONCLUSIONS

The results of gravity and microearthquake surveys in the Chinshan-Tanshui area can be summarized as follows:

- (1) The Chinshan fault is a thrust fault. Its plane dips to the southeast with a angle of about 55 to 60 *degrees*.
- (2) The seismicity in the study area is not very active. Although the general pattern of epicenter distribution is dispersed without a clear correlation with existing individual faults in the area, the hypocentral profiles perpendicular to the Chinshan fault demonstrate some correlation between the seismicity and the Chinshan fault.
- (3) Most earthquakes occurred at depths shallow than 10 *km*, obviously condensing in the zone from the surface to the 5 *km* depth.
- (4) The result of the composite fault plane solutions indicate that most of the focal mechanism are normal fault. It is probably corresponding to the geothermal activities of the Tatun or Chihsinshan Volcanos.

*Acknowledgements.* The authors are grateful to their colleagues Messrs. Horng-Yuan Yen, Cheng-Horng Lin, Wei-Chang Huang, Wo-Lung Lee and Teh-Ang Lee for participation in field work and assistance in data processing. We thank the TTSN group of our institute for providing part of earthquake data. Thanks are also due to Ms. Huei-Fen Chiu for preparing the drawings. This study was supported by the National Science Council of the Republic of China Grant Nos. NSC77-0414-P001-04B.

## REFERENCES

- Chang, Stanley, S. L., 1968: Regional stratigraphic study of the Lower Miocene Formations in northern Taiwan: *Petrol. Geol. Taiwan* 6, 47-70.
- Chou, J. T., 1962: Stratigraphic and sedimentary study of the Mushan Formation in northern Taiwan: *Petrol. Geol. Taiwan, Mr King's Jubilee*, Volume (1), 87-119.
- Geiger, L., 1912: Probability method for the determination of earthquake epicenters from the arrival time only: *Bull. St. Louis Univ.* 8, 60-71.
- Hammer, S., 1939: Terrain correction for gravimeter stations: In "*Applied Geophysics*", ed by Telford W. M. *et al.*, 860 p.
- Hsieh, S. H. and C. C. Hu, 1972: Gravimetric and magnetic studies of Taiwan: *Petrol. Geol. Taiwan* 10, 283-321.
- Ho, C. S., 1975: *An introduction to geology of Taiwan-explanatory text of the geologic map of Taiwan*: The Ministry of Economic Affairs, Taipei, Taiwan, R. O. C., 153 p.

- Hsu, M.-Y., 1967: Geology of the coal field between Chinshan and Shihmen, northern Taiwan, *Bull. Geol. Surv. Taiwan*, **19**, 15-26 (Chinese), 9-14 (English).
- Hsu, T. L. and H. C. Chang, 1979: Quaternary faulting in Taiwan: *Mem. Geol. Soc. China*, **3**, 155-165.
- Hsu, T. L., 1981: Geological map of Taiwan, Linkou sheet, Sanchih sheet, and Taipei sheet, *Geol. Surv. ROC*.
- Lee, W. H. K. and L. C. Lahr, 1972: HYPO71: A computer program for determining hypocenter, magnitude, and first motion pattern of local earthquakes: *USGS Open File Rep.*, 100 p.
- , R. E. Bennett, and K. L. Meagher, 1972: A method of estimating magnitude of local earthquakes from signal duration: *U. G. Geol. Surv. Open File Rep.*, 100 p.
- Regan, R. D., and W. J. Hinze, 1976: The effect of finite data length in the spectral analysis of ideal gravity anomalies, *Geophysics*, **41**, 44-55.
- Talwani, M., J. L. Worzel and M. Landsman, 1959: Rapid gravity computations for the two-dimensional bodies with application to the Mendocino submarine fracture zone: *J. Geophys. Res.* **64**, 49-59.
- Tsai, Y. B., C. C. Feng, J. M. Chiu and H. B. Liaw, 1975: Correlation between microearthquakes and geologic faults in the Hsintien-Ilan area: *Petrol. Geol. Taiwan* **12**, 149-167.
- Yeh, Y. H., 1986: Three dimensional crustal and upper mantle structures of northern Taiwan from earthquake and gravity data: *Ph. D thesis, National Central Univ.*, 142 p.
- , W. H. Wang, H. Y. Yen and Y. B. Tsai, 1984: Subsurface structures in the Minghsiung-Meishan area, southwestern Taiwan from gravity anomaly data: *Bull. Inst. Earth Sci., Academia Sinica* **4**, 101-116.

# 金山淡水地區重力與微震研究

陳光榮 葉義雄

中央研究院地球科學研究所

## 摘要

本研究係利用精密重力及微震調查方法，於金山淡水之間（東經 $121^{\circ}23' \sim 121^{\circ}43'$ ，北緯 $25^{\circ}0' \sim 25^{\circ}20'$ ）進行測勘，以期瞭解本地區斷層之分佈範圍與性質。在重力方面，共取了二條大致垂直於金山斷層走向的測線。所得之重力資料經模擬過程來推求該測線下的地下地質構造，結果顯示金山斷層及新莊斷層皆為逆衝斷層，分別向東南傾斜約 $55^{\circ}$ 至 $60^{\circ}$ 。從十二個測站的臨時測震網，搜集了五十八天完整記錄，一共定出發生於本地區內規模從0.2~3.2的地震計223次，大部份淺於10公里。由二十一個合成斷層面解的結果，顯示此地區之地震機制大都為正斷層型態，這些地震應與本地區內大屯山及七星山區地熱活動有關。中央研究院地球科學研究所的臺灣區測震網（TTSN）在過去十三年間（1973-1985）測定到發生於本地區之地震共計433次，它們的震央分佈型態與臨時測震網所測得的非常相近。一般而言，本地區的地震活動並不是十分活躍的。